Available online at www.sciencedirect.com
ScienceDirect
Trans. Nonferrous Met. Soc. China 23(2013) 3180−3185
Transactions of Nonferrous Metals Society of China
www.tnmsc.cn

Hot deformation behavior of extruded AZ80 magnesium alloy

Hui-zhong LI[1,2,3], Xiao-yan WEI[1], Jie OUYANG[1], Jun JIANG[1], Yi LI[1]

1. School of Materials Science and Engineering, Central South University, Changsha 410083, China;
2. State Key Laboratory of Powder Metallurgy, Central South University, Changsha 410083, China;
3. Key Laboratory of Nonferrous Metal Materials Science and Engineering of Ministry of Education, Central South University, Changsha 410083, China

Received 24 January 2013; accepted 24 June 2013

Abstract: The hot deformation behavior of extruded AZ80 magnesium alloy was studied through hot compression tests performed at temperatures ranging from 250 to 450 °C with strain rates varying from 0.001 to 10 s^{-1}. The flow stress was corrected due to the deformation heating. The Zener−Hollomon parameter (*Z* parameter) and processing map were established to describe the hot deformation behavior. The results indicate that the applicable deformation should be conducted at the strain rate of 0.1 s^{-1} and the temperature range of 350−400 °C. Besides, the relationship between the microstructure evolution and *Z* parameter was also discussed. High temperature and low strain rate result in a low *Z* parameter, which leads to full dynamic recrystallization (DRX) and large DRX grain size in the microstructure. Considering processing map and microstructure, the hot deformation should be carried out at the temperature of 400 °C and the strain rate of 0.1 s^{-1}.

Key words: AZ80 magnesium alloys; hot deformation; processing map; *Z* parameter

1 Introduction

Due to the advantages such as high strength and low price, AZ80 magnesium alloy becomes a commercial alloy and therefore great attention is paid to it by many researchers and scientists [1−3]. However, it exhibits poor workability at room temperature because of the hexagonal close-packed crystal structure [4]. Consequently, hot deformation process which can activate non-basal slips is applied to it [5]. A number of studies have been carried out on the hot workability of Mg−Al−Zn alloys [6−9]. Researchers investigated the effect of initial grain size on dynamic recrystallization (DRX) [10] and study shows that initial grain size has little influence. However, *Z* parameter has great impact on DRX grains. *Z* parameter is related to mechanisms of DRX, grain boundary strengthening and twinning and causes different DRX grain sizes. There are also some other related research hotspots. For example, LOU et al [11] reported the extensive cross slips near grain boundaries and abundant twins at the early stages of plastic flow in AZ80 magnesium alloy during DRX.

Many studies were carried on as-cast Mg−Al−Zn magnesium alloys. But deformation of some machine components made of AZ80 magnesium alloy will usually be conducted by die forging. In order to improve the workability of die forging, blanks need to be pre-deformed through extrusion and open die forging. In this study, extruded AZ80 magnesium alloy is used in the compression experiments so that it accords with the die forging process. The aim of this study is to establish *Z* parameter and processing map of extruded AZ80 magnesium alloy and observe the microstructure under different deformation conditions, therefore the hot deformation condition for extruded AZ80 magnesium alloy can be determined.

2 Experimental

The initial material was the extruded AZ80 magnesium rod with a diameter of 110 mm. The initial microstructure is shown in Fig. 1. Obviously, full recrystallization occurred and the average grain size was about 20 μm. Cylindrical specimens were machined along the extrusion direction from the extruded rod to a height of 12 mm and a diameter of 8 mm. The hot compression tests were conducted on a Gleeble−1500

Corresponding author: Hui-zhong LI; Tel: +86-731-88830377; E-mail: lhz606@csu.edu.cn
DOI: 10.1016/S1003-6326(13)62850-2

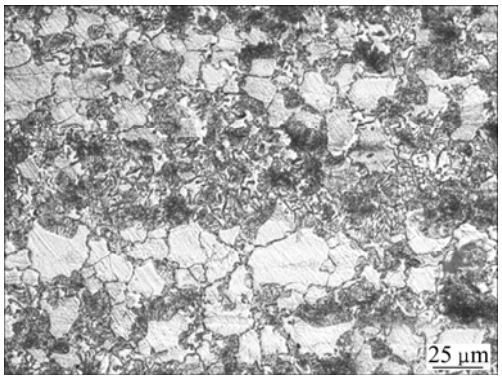

Fig. 1 Initial optical microstructure of extruded AZ80 magnesium alloy

thermo-mechanical simulator. Specimens were heated to a pre-set temperature within 60 s, held for 3 min and then compressed to a total true strain of 0.7 at temperatures ranging from 250 to 450 °C and strain rates from 0.001 to 10 s^{-1}. The graphite lubricant was applied to specimens and platens. The microstructure was observed in the longitudinal section of compressed specimen using an optic microscope (OM) and transmission electron microscope (TEM). The specimens for OM were grounded, polished and etched in an acetic picral solution containing picric acid. The specimens for TEM were ground, twin-jet electropolished and observed using TecnaiG^{2}20 and JEM−2100F TEM.

3 Results

3.1 True stress—strain curves

Deformation heating results in a higher temperature than the pre-set one, which leads to a lower flow stress than the actual stress under isothermal conditions. Therefore, it is necessary for experimental data to be corrected. The temperature increase is calculated as

$$\Delta T=\frac{0.95\eta\int\sigma\mathrm{d}z}{\rho c_p} \tag{1}$$

where η is the adiabatic correction factor, $\int\sigma\mathrm{d}\varepsilon$ is the mechanical work, ρ is the density, c_p is the specific heat capacity, and ρc_p is the heat capacity or volume specific heat capacity. The adiabatic correction is the same as the report by LIANG et al [12].

Taking deformation heating into consideration, the true stress—strain curves under different conditions are shown in Fig. 2. The full lines represent the uncorrected curves and the dotted lines represent the corrected curves. The stress—strain curves show a typical flow behavior of DRX. The occurrence of DRX is recognized by the peak due to the dynamic softening effect [13,14]. At lower strain rates of 0.001 and 0.01 s^{-1}, the stress undergoes a peak stress and decreases gradually. Since time is limited for recrystallization nucleation and grain growth, the stress peak is less obvious at a higher strain rate. Besides, an increase in strain rate or a decrease in temperature causes an increment in peak strain, while a decrease in temperature or an increase in strain rate leads to an increase in peak stress. Apparently, the flow stress is sensitive to strain rate and temperature.

3.2 *Z* parameter

Z parameter correlates flow stress, strain rate and temperature and can be calculated as [15]

$$Z=\dot{\varepsilon}\exp\left[\frac{Q}{RT}\right]=f(\sigma)=\begin{cases}A_1\sigma^{n'}, & \alpha\sigma<0.8\\ A_2\exp(\beta\sigma), & \alpha\sigma\geq1.2\\ A[\sinh(\alpha\sigma)]^n, & \text{for all }\sigma\end{cases} \tag{2}$$

where $\dot{\varepsilon}$ is the strain rate, σ is the peak stress, n is the stress exponent, Q is the activation energy, R is the gas mole constant, T is the thermodynamic temperature, $\alpha(\approx\beta/n')$ is the stress multiplier, and A_1, A_2, A, n' and β are the material parameters. The power law description is suitable for creep with low stress. The exponential law is perfect at high strain rates and low temperatures. In a wide range of stress, the hyperbolic sine law is the proper equation. Taking natural logarithms of equation (2), the following expressions can be derived:

$$\ln Z=\ln A+n\ln[\sinh(\alpha\sigma)] \tag{3}$$

By calculation, the values of α, n and A are 0.008, 5.324 and 22.360, respectively. By substituting all the parameters, $\ln Z$ can be obtained as

$$\ln Z=22.360+5.324\ln[\sinh(0.008\sigma)] \tag{4}$$

$\ln Z$ is linear with respect to $\ln[\sinh(\alpha\sigma)]$, as shown in Fig. 3.

3.3 Processing map

Based on the dynamic materials model, processing maps contribute to evaluating the microstructure of material with different processing parameters [16]. Processing maps consist of power dissipation efficiency map and instability map. The efficiency of power dissipation (η') is defined as [17]

$$\eta'=\frac{2m}{m+1} \tag{5}$$

Strain rate sensitivity (m) is defined as

$$m=\left(\frac{\partial J}{\partial G}\right)_{\varepsilon,T}=\left(\frac{\partial\ln\sigma}{\partial\ln\varepsilon}\right)_{\varepsilon,T} \tag{6}$$

where G is the power dissipated in plastic work (most converted to heat) and J is the dissipater power co-content related to metallurgical mechanism. Generally, the relationship between stress σ and strain rate $\dot{\varepsilon}$ can be described as

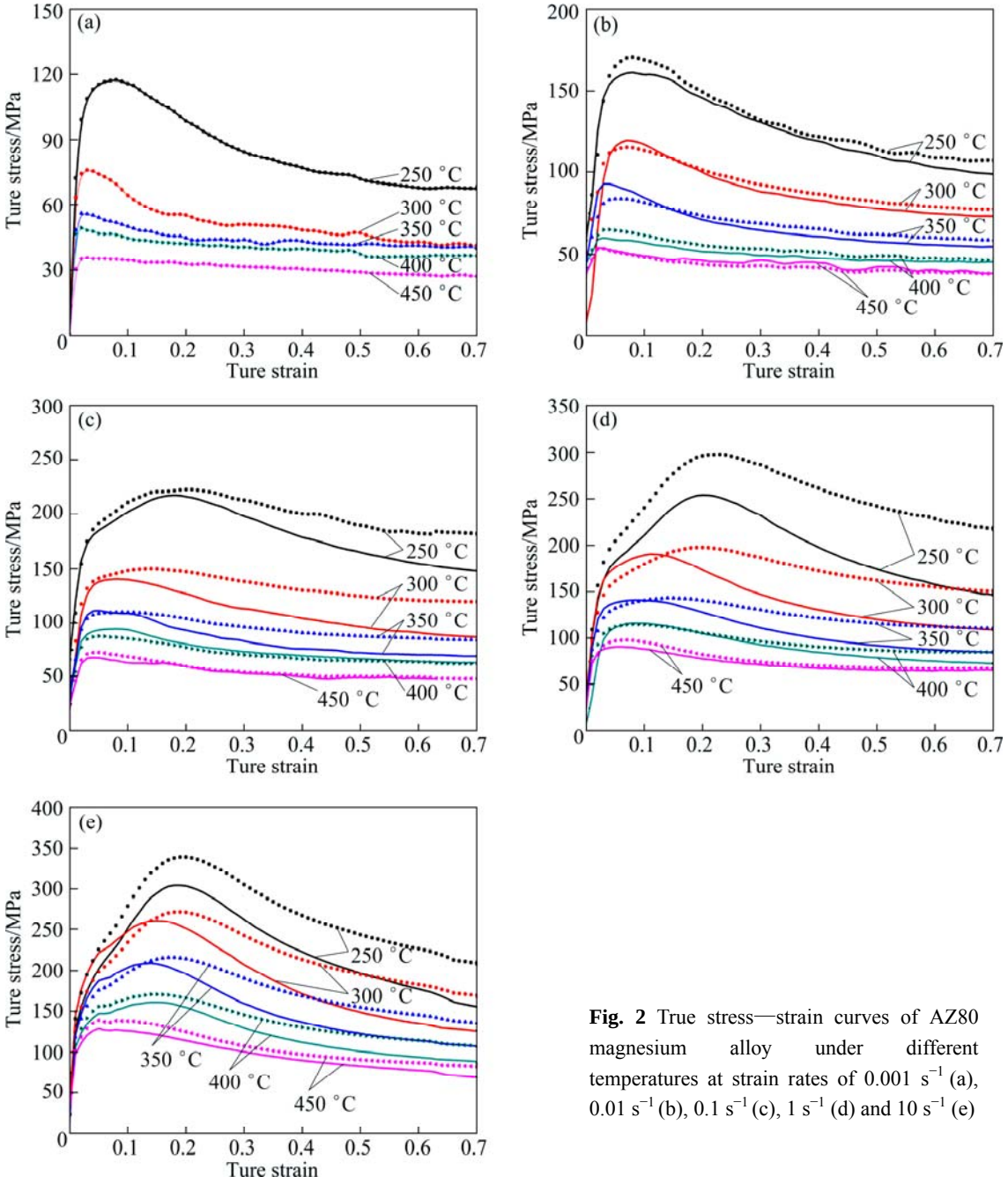

Fig. 2 True stress—strain curves of AZ80 magnesium alloy under different temperatures at strain rates of 0.001 s^{-1} (a), 0.01 s^{-1} (b), 0.1 s^{-1} (c), 1 s^{-1} (d) and 10 s^{-1} (e)

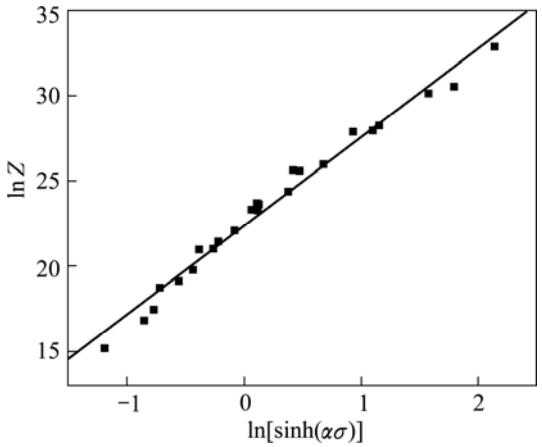

Fig. 3 Plot of ln Z against ln[sinh($\alpha\sigma$)]

$$\ln\sigma = a + b\ln\dot{\varepsilon} + c(\ln\dot{\varepsilon})^2 + d(\ln\dot{\varepsilon})^3 \tag{7}$$

In the power dissipation efficiency map, different domains represent different mechanisms, such as dynamic recovery, DRX, void formation, wedge cracking and intercrystalline cracking. As for the instability map, the dimensionless parameter ξ is derived by instability criterion and defined as [18]

$$\xi = \frac{\partial \ln\left(\frac{m}{m+1}\right)}{\partial \ln\dot{\varepsilon}} + m \le 0 \tag{8}$$

In regions with negative ξ, flow instabilities such as adiabatic shear bands and flow localizations occur.

The processing maps of as-extruded AZ80 magnesium alloy obtained at strains of 0.1, 0.3, 0.5 and 0.7 are presented in Figs. 4(a)−(d), respectively. The efficiency of power dissipation is presented by the counter number and the shaded regions indicate the flow instability. Obviously, processing map is significantly influenced by strain. Different strains lead to different domains of flow instability. At the strain of 0.1, flow instability occurs at temperature below 350 °C. As strain reaches 0.3−0.5, the flow instability occurs at high strain rates. As strain reaches 0.7, flow instability also occurs at temperatures higher than 375 °C, mainly at both high strain rates and low strain rates. The power dissipation efficiency generally decreases with increasing strain, especially at high strain rates. Besides, power dissipation efficiency varies dramatically with strain rate at lower temperatures but changes slightly at high temperatures. The peak power dissipation efficiency is almost equal to 0.45 at 300 °C and strain rate of 0.001 s^{-1} at different strains.

Considering both the power dissipation efficiency and stability, thermal deformation of AZ80 alloy should be conducted at the temperatures of 350−400 °C with the strain rate of 0.1 s^{-1}.

3.4 Microstructure evolution

Figure 5 shows the microstructure of extruded AZ80 magnesium alloy after hot compression under different deformation conditions. The volume fraction and grain size of DRX are significantly affected by the deformation temperature and strain rate, which directly determines the Z value according to Eq. (2). At high temperatures and low strain rates, the value of Z is relatively low while Z value is higher at low temperatures and high strain rates. Figures 5(a)−(e) indicate the microstructure evolution of extruded AZ80 magnesium alloy at the strain rate of 0.1 s^{-1} at different temperatures. At a certain strain rate, an increase in temperature contributes to decreasing Z value, and a more adequate proceeding of DRX and a larger volume fraction of DRX grain can be observed. Figures 5(e) and (f) show the microstructure evolution at the temperature of 450 °C with the strain rates of 0.1 s^{-1} and 0.01 s^{-1}, respectively. Obviously, a lower strain rate results in a lower Z value, which leads to more completed DRX and a larger grain size. At 400 °C and 0.1 s^{-1}, complete DRX can be observed, which is supposed to be the best deformation condition. At 450 °C and 0.01 s^{-1}, Z value is very low, the DRX grains coarsen significantly and the grain size is generally very large.

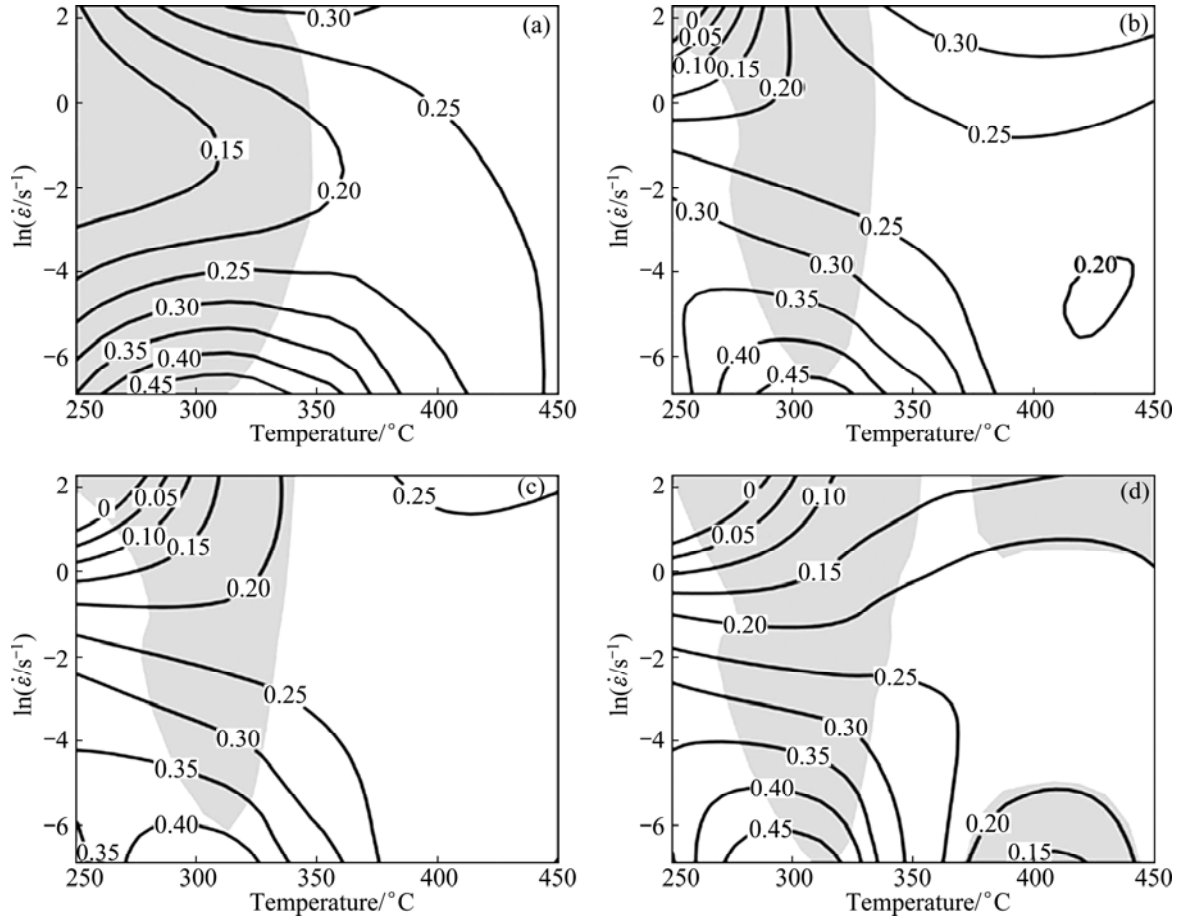

Fig. 4 Processing maps at strains of 0.1 (a), 0.3 (b), 0.5 (c) and 0.7 (d)

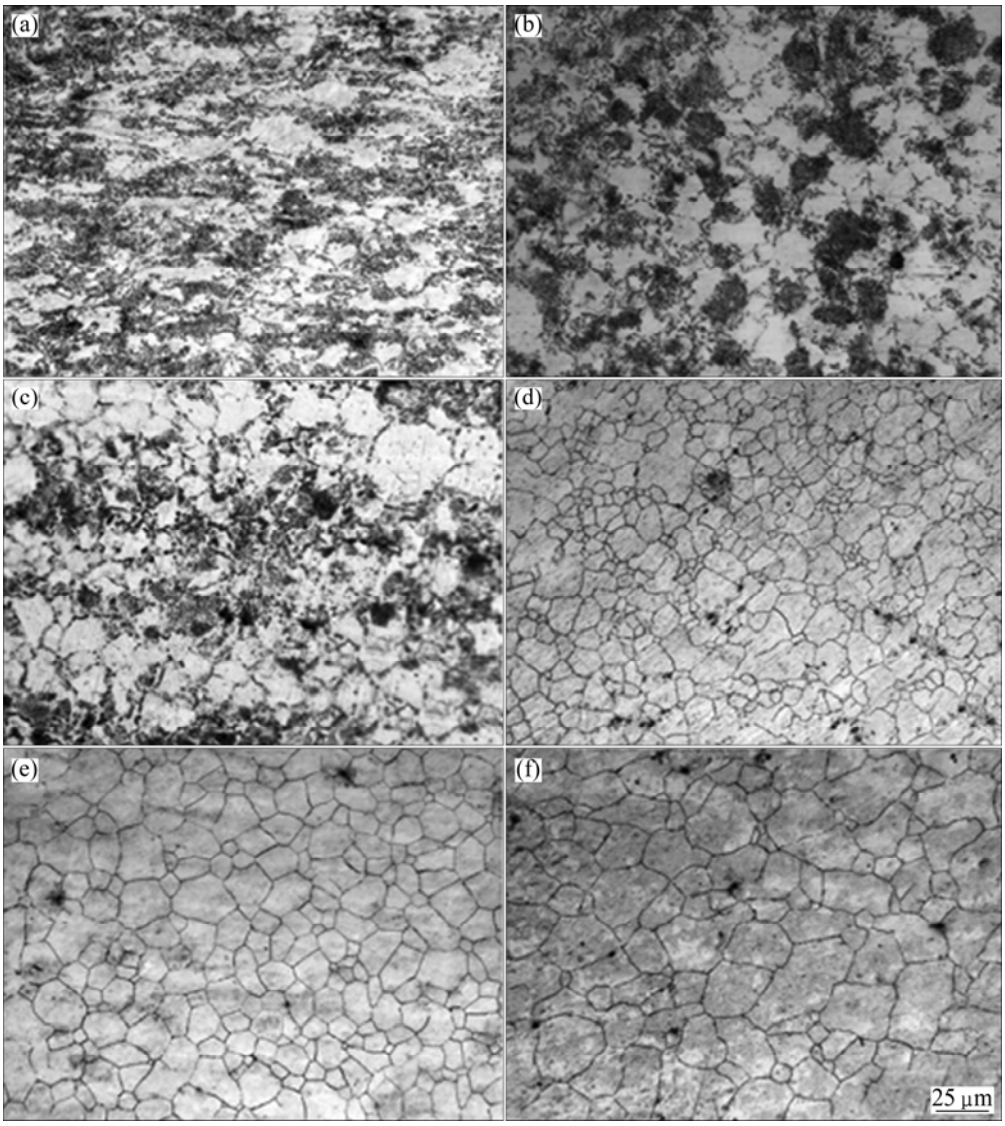

Fig. 5 Optical microstructures of extruded AZ80 Mg alloy under different deformation conditions: (a) 250 °C, 0.1 s^{-1}; (b) 300 °C, 0.1 s^{-1}; (c) 350 °C, 0.1 s^{-1}; (d) 400 °C, 0.1 s^{-1}; (e) 450 °C, 0.1 s^{-1}; (f) 450 °C, 0.01 s^{-1}

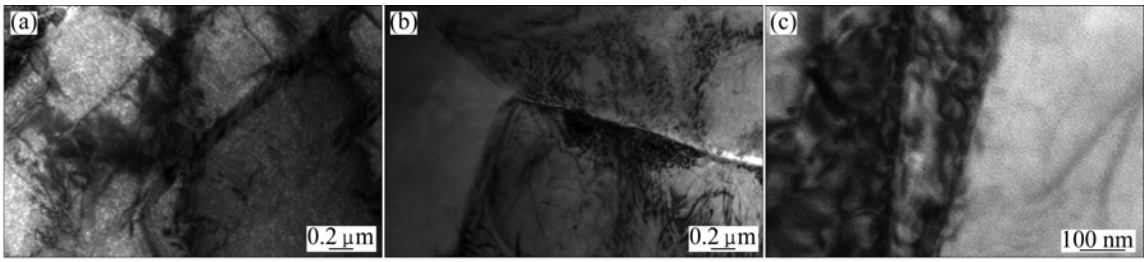

Fig. 6 TEM images of extruded AZ80 magnesium alloy compressed at 300 °C and 0.001 s^{-1}: (a) Dislocations around twin; (b) Dislocations around boundary; (c) Sub-grain around twin

Figure 6 shows the TEM images of extruded AZ80 magnesium alloy. In Figs. 6(a) and (b), dislocations around twin and grain boundary can be both observed. In Fig. 6(c), sub-grains are formed around twin. CHANGIZIAN et al [19] reported that the initial grains can be divided by twins and denser dislocation tangles around twins can provide favorable sites to form sub-grains with low-angle grain boundaries, which will grow into new DRX grains with large-angle grain boundaries. The observation indicates the mechanism of twin dynamic recrystallization in magnesium alloys and accords with the previous report [19].

4 Conclusions

1) The Z parameter for extruded AZ80 magnesium alloy can be expressed as $\ln Z = 22.360 + 5.324\ln[\sinh(0.008\sigma)]$.

2) Efficiency of power dissipation stays relatively gently at high temperatures. The instability usually occurs at temperature lower than 350 °C. The hot deformation conditions for extruded AZ80 magnesium alloy are the temperature of 400 °C and the strain rate of 0.1 s^{-1}.

References

[1] LI Zhao-zhi, YANG Ya-qin, ZHANG Zhi-min. Transformation mechanism of lamellar microstructure of AZ80 wrought Mg alloy during warm deformation [J]. Transactions of Nonferrous Metals Society of China, 2008, 18(S1): s156−s159.

[2] ZHAO Gao-zhan, YANG Lin, DUAN Xun-xing, REN Xiao-hua, ZHU Li-min, YANG Ting-jun, GUO Xiang-yong, HAO Shao-nan. Microstructure evolution and mechanical properties of AZ80 alloy reheated from as-cast and deformed states [J]. Transactions of Nonferrous Metals Society of China, 2012, 22(S2): s450−s456.

[3] LI Yan, ZHANG Zhi-min, XUE Yong. Influence of aging on microstructure and mechanical properties of AZ80 and ZK60 magnesium alloys [J]. Transactions of Nonferrous Metals Society of China, 2011, 21(4): 739−744.

[4] ZHANG J, FANG C, YUAN F, LIU C. A comparative analysis of constitutive behaviors of Mg−Mn alloys with different heat-treatment parameters [J]. Materials Design, 2011, 32(4): 1783−1789.

[5] TAN Cheng-wen, XU Shan-na, WANG Lu, CHEN Zhi-yong, WANG Fu-chi, CAI Hong-nian. Effect of temperature on mechanical behavior of AZ31 magnesium alloy [J]. Transactions of Nonferrous Metals Society of China, 2007, 17(1): 41−45.

[6] XU Hong-yan, WANG Qiang, ZHANG Zhi-min. Effect of thermal processing on microstructure and mechanical properties of AZ80 magnesium alloy [J]. Transactions of Nonferrous Metals Society of China, 2008, 18(S1): s122−s126.

[7] LÜ Wen-quan, QUAN Guo-zheng, YU Chun-tang, ZHAO Lei, ZHOU Jie. Effect of strain, strain rate and temperature on workability of AZ80 wrought magnesium alloy [J]. Transactions of Nonferrous Metals Society of China, 2012, 22(S3): s650−s655.

[8] SLOOFF F A, DZWONCZYK J S, ZHOU J, DUSZCZYK J, KATGERMAN L. Hot workability analysis of extruded AZ magnesium alloys with processing maps [J]. Materials Science and Engineering A, 2010, 527(3): 735−744.

[9] SRINIVASAN N, PRASAD Y V R K, RAO P R. Hot deformation behaviour of Mg−3Al alloy—A study using processing map [J]. Materials Science and Engineering A, 2008, 476(1−2): 146−156.

[10] BEER A G, BARNETT M R. Influence of initial microstructure on the hot working flow stress of Mg−3Al−1Zn [J]. Materials Science and Engineering A, 2006, 423(1−2): 292−299.

[11] LOU Y, LI L, ZHOU J, NA L. Deformation behavior of Mg−8Al magnesium alloy compressed at medium and high temperatures [J]. Materials Characterization, 2011, 62(3): 346−353

[12] LIANG X, LIU Y, LI H, ZHOU C, XU G. Constitutive relationship for high temperature deformation of powder metallurgy Ti−47Al−2Cr−2Nb−0.2W alloy [J]. Materials Design, 2012, 37: 40−47.

[13] McQWEEN H J. Development of dynamic recrystallization theory [J]. Materials Science and Engineering A, 2004, 387−389: 203−208.

[14] POLIAK E I, JONAS J J. A one-parameter approach to determining the critical conditions for the initiation of dynamic recrystallization [J]. Acta Materialia, 1996, 44(1): 127−136.

[15] MANDAL S, RAKESH V, SIVAPRASAD P V, VENUGOPAL S, KASIVISWANATHAN K V. Constitutive equations to predict high temperature flow stress in a Ti-modified austenitic stainless steel [J]. Materials Science and Engineering A, 2009, 500(1−2): 114−121.

[16] PRASAD Y V R K. Processing maps: A status report [J]. Journal of Materials Engineering and Performance, 2003, 12(6): 638−645.

[17] RAJAMUTHAMILSELVAN M, RAMANATHAN S, KARTHIKEYAN R. Processing map for hot working of SiC_p/7075 Al composites [J]. Transactions of Nonferrous Metals Society of China, 2010, 20(4): 668−674.

[18] ZIEGLER H. Progress in solid mechanics [M]. Vol 4. New Jersey: Wiley Press, 1963: 93.

[19] CHANGIZIAN P, ZAREI-HANZAKI A, ABEDI H R. On the recrystallization behavior of homogenized AZ81 magnesium alloy: The effect of mechanical twins and γ precipitates [J]. Materials Science and Engineering A, 2012, 558: 44−51.

挤压态 AZ80 镁合金的热变形行为

李慧中[1,2,3]，卫晓燕[1]，欧阳杰[1]，姜 俊[1]，李 轶[1]

1. 中南大学 材料科学与工程学院，长沙 410083；
2. 中南大学 粉末冶金国家重点实验室，长沙 410083；
3. 中南大学 有色金属材料科学与工程教育部重点实验室，长沙 410083

摘 要：通过热压缩实验，研究挤压态 AZ80 镁合金在变形温度为 250~450 °C，应变速率为 0.001~10 s^{-1} 条件下的热变形行为。采用经过温升修正的流变应力计算该合金的 Zener−Hollomon 参数(Z 参数)。结果表明，挤压态 AZ80 镁合金适宜的变形条件为应变速率 0.1 s^{-1}、变形温度 350~400 °C。另外，讨论了显微组织演化与 Z 参数之间的关系。在高温及低应变速率(低 Z 参数)时，合金发生了完全再结晶并产生了大的再结晶晶粒。综合考虑加工图和显微组织，变形温度 400 °C、应变速率 0.1 s^{-1} 是合金适宜的热变形条件。

关键词：AZ80 镁合金；热变形；加工图；Z 参数

(Edited by Xiang-qun LI)